Sciencexpress Report

The Plant Cell Wall–Decomposing Machinery Underlies the Functional Diversity of Forest Fungi

Daniel C. Eastwood,[1]*†‡ Dimitrios Floudas,[2]† Manfred Binder,[2]† Andrzej Majcherczyk,[3]† Patrick Schneider,[4]† Andrea Aerts,[5] Fred O. Asiegbu,[6] Scott E. Baker,[7] Kerrie Barry,[5] Mika Bendiksby,[8] Melanie Blumentritt,[9] Pedro M. Coutinho,[10] Dan Cullen,[11] Ronald P. de Vries,[12] Allen Gathman,[13] Barry Goodell,[9,14] Bernard Henrissat,[10] Katarina Ihrmark,[15] Hävard Kauserud,[16] Annegret Kohler,[17] Kurt LaButti,[5] Alla Lapidus,[5] José L. Lavin,[18] Yong-Hwan Lee,[19] Erika Lindquist,[5] Walt Lilly,[13] Susan Lucas,[5] Emmanuelle Morin,[17] Claude Murat,[17] José A. Oguiza,[18] Jongsun Park,[19] Antonio G. Pisabarro,[18] Robert Riley,[5] Anna Rosling,[15] Asaf Salamov,[5] Olaf Schmidt,[20] Jeremy Schmutz,[5] Inger Skrede,[16] Jan Stenlid,[15] Ad Wiebenga,[12] Xinfeng Xie,[9] Ursula Kües,[3]* David S. Hibbett,[2]* Dirk Hoffmeister,[4]* Nils Högberg,[15]* Francis Martin,[17]* Igor V. Grigoriev,[5]* Sarah C. Watkinson[21]*

[1]College of Science, University of Swansea, Singleton Park, Swansea SA2 8PP, UK. [2]Biology Department, Clark University, Worcester, MA 01610, USA. [3]Georg-August-University Göttingen, Büsgen-Institute, Büsgenweg 2, 37077 Göttingen, Germany. [4]Friedrich-Schiller-Universität, Hans-Knöll-Institute, Beutenbergstrasse 11a, 07745 Jena, Germany. [5]US Department of Energy Joint Genome Institute, Walnut Creek, CA, USA. [6]Department of Forest Sciences, Box 27, FI-00014, University of Helsinki, Helsinki, Finland. [7] Pacific Northwest National Laboratory, 902 Battelle Boulevard, P.O. Box 999, MSIN P8-60, Richland, WA 99352, USA. [8]Natural History Museum, University of Oslo, PO Box 1172, Blindern, NO-0138, Norway. [9]Wood Science and Technology, University of Maine, Orono, ME, USA. [10]UMR 6098 CNRS-Universités Aix-Marseille I& II, 13288 Marseille Cedex 9, France. [11]Forest Products Laboratory, Madison, WI 53726, USA. [12]CBS-KNAW Fungal Biodiversity Centre, Uppsalalaan 8, 3584 CT Utrecht, The Netherlands. [13]Department of Biology, Southeast Missouri State University, Cape Girardeau, MO, USA. [14]Department of Wood Science and Forest Products, 230 Cheatham Hall, Virginia Tech. Blacksburg, VA 24061, USA. [15]Swedish University of Agricultural Sciences, S-750 07 Uppsala, Sweden. [16]Department of Biology, University of Oslo, P.O. Box 1066 Blindern, N-0316 Oslo, Norway. [17]UMR 1136, INRA-Nancy Université, Interactions Arbres/Microorganismes, INRA-Nancy, 54280 Champenoux, France. [18]Public University of Navarre, 31006 Pamplona, Spain. [19]Department of Agricultural Biotechnology, Seoul National University, Seoul, 151*921. [20]University of Hamburg, Leuschnerstr. 91, D-21031 Hamburg, Germany. [21]Department of Plant Sciences, University of Oxford, Oxford, OX1 3RB, UK.

*These authors contributed equally to this work as senior authors.

†These authors contributed equally to this work as first authors.

‡To whom correspondence should be addressed. E-mail: d.c.eastwood@swansea.ac.uk

Brown rot decay removes cellulose and hemicelluloses from wood, residual lignin contributing up to 30% of forest soil carbon, and is derived from an ancestral white rot saprotrophy where both lignin and cellulose are decomposed. Comparative and functional genomics of the "dry rot" fungus *Serpula lacrymans*, derived from forest ancestors, demonstrated that the evolution of both ectomycorrhizal biotrophy and brown rot saprotrophy were accompanied by reductions and losses in specific protein families, suggesting adaptation to an intercellular interaction with plant tissue. Transcriptome and proteome analysis also identified differences in wood decomposition in *S. lacrymans* relative to the brown rot *Postia placenta*. Furthermore, fungal nutritional mode diversification suggests that the boreal forest biome originated via genetic coevolution of above and belowground biota.

Many Agaricomycete fungi have been sequenced to date (*1*) permitting comparative and functional genomic analyses of nutritional niche adaptation in the underground fungal networks that sustain boreal, temperate, and some sub-tropical forests (*2*). Through the sequencing of the brown rot wood decay fungus *S. lacrymans*, we conducted genome comparisons with sequenced fungi including species representing each of a range of functional niches: brown rot and white rot wood decay, parasitism and mutualistic ectomycorrhizal symbiosis.

Only 6% of wood decay species are brown rots (*3*) but, being associated with conifer wood (*4*), they dominate decomposition in boreal forests. Their lignin residues contribute up to 30% of carbon in the organic soil horizons (*5*). Long-lived (*6*), and with capacity to bind nitrogen and cations (*7*), these phenolic polymers condition the nutrient-poor acidic soils of northern conifer forests.

Brown rot wood decay involves an initial non-enzymic attack on the wood cell wall (*8*) generating hydroxyl radicals (·OH) extracellularly via the Fenton reaction:

$$Fe^{2+} + H_2O_2 + H^+ \rightarrow Fe^{3+} + \cdot OH + H_2O$$

Hydrogen peroxide is metabolically generated by oxidase enzymes, e.g. glyoxal oxidases and copper radical oxidases. The hydroxyl radical has a half life of nanoseconds (*8*) and is the most powerful oxidising agent of living cells. However, we do not know how it is spatially and temporally targeted to wood cell wall components. Divalent iron is scarce in aerobic environments where the fungus is obligate and the trivalent ion is energetically favored. Phenolates synthesised by brown rot fungi, including *S.lacrymans* (*9*), can reduce Fe^{3+} to Fe^{2+}. Such phenolates may be modified lignin derivatives or fungal metabolites (*10*). Following initial bond breakages in the cellulose chain, side chain hemicelluloses (arabinan, galactan) are removed, followed by main chains (xylan, mannan (*11*), with subsequent hydrolysis of cellulose by synergistic glycoside hydrolases. Residual lignin is demethylated. White rot fungi, by contrast, decompose both cellulose and lignin, with free radical attack theorized to break a variety of bonds in the lignin phenylpropanoid heteropolymer.

S. lacrymans is in the Boletales, along with several ectomycorrhizal lineages (Fig. 1A) (*12*). *S. lacrymans* is thus phylogenetically distant from brown rot *P. placenta (Polyporales)* (*13*), as well as other sequenced ectomycorrhizal fungi (*14*, *15*), parasites, and white rot wood decomposers (*16*). We estimated divergence dates in fungal phylogeny using the data set of Binder *et al.* (2010) (*17*) [supporting online material (SOM), molecular clock analyses], with two well-characterized fungal fossils used to calibrate the minimum ages of the marasmioid (node 10 in fig 1A) and suilloid clades (Fig, 1A, node 11). The estimated age of the split between *Serpula* and its ectomycorrhizal sister-group *Austropaxillus* (53.1-15 Mya) (Fig 1A and table S11) suggests that transition from brown rot saprotrophy to mutualistic symbiosis occurred after rosids (Eurosids I) became widespread (Fig. 1A) (*18*). Diversification in fungal nutritional modes occurred alongside diversification of angiosperms and gymnosperms, as these fungi are currently associated with members of both gymnosperms (Pinaceae) and angiosperms (*18*).

S. lacrymans comprises two subgroups, *S. lacrymans* var *shastensis*, found in montane conifer forest, and *S. lacrymans* var *lacrymans*, cause of building dry rot, which diverged in historic time (*19*). Two *S. lacrymans* var *lacrymans* complementary monokaryons (haploids of strain S7), S7.9 (A2B2) and S7.3 (A1B1) (*20*) were sequenced via Sanger and 454 pyro-sequencing, respectively. The genome of *S. lacrymans* S7.9 was 42.8 Mbp, containing 12,917 gene predictions. For methodology, genome analysis and annotation, see supplementary materials (*21*).

We analysed 19 gene families of enzymes for lignocellulose breakdown: carbohydrate active enzymes [CAZy, http://www.cazy.org (*22*)] (glycoside hydrolases and carbohydrate esterases) and oxidoreductases (table S9). Losses and expansions in these families were compared across 10 fungi including Agaricomycetes with a range of nutritional modes (Fig. 1, B and C, and table S9). Convergent changes in enzyme complement were found in the two independently-evolved brown rot species, with parallels in the ectomycorrhizal *Laccaria bicolor* (fig S3, table S9). The inferred most recent common ancestor of the Agaricales, Boletales and Polyporales is predicted to be a white rot with 66 to 83 hydrolytic CAZy genes and 27-29 oxidoreductases (Fig 1, B and C). Brown rot and ectomycorrhizal fungi have the fewest hydrolytic CAZy genes. Brown rot fungi have fewest oxidoreductases, due, not to gene losses, but to gene duplications in white rot species.

Both brown rot and ectomycorrhizal fungi lacked class II peroxidases, used by white rot fungi in depolymerising the non-utilisable lignin matrix of wood to unmask utilisable cellulose embedded within it. This family was expanded in the white rots *Coprinopsis cinerea, Phanerochaete chrysosporium* and *Schizophylum commune*, with 29, 43 and 24 genes respectively, with only 19 each in *S.lacrymans* and *P. placenta*. Oxidoreductases conserved in brown rot fungi included iron and quinone reductases, and multicopper oxidases (fig. S3 and table S8). Absence of ligninolysis in brown rots raises the question of how they achieve pervasive cellulolysis in wood with the lignin matrix intact.

Glycoside hydrolase (GH) gene families had parallel patterns of losses and expansion in both brown rots and ectomycorrhizas. CAZy families GH5 (endoglucanases, hydrolysing cellulose) and GH28 (pectinases, hydrolysing intercellular cohesive polysaccharides in plant tissues) were expanded in both brown rot species, where they might facilitate intercellular enzyme diffusion, and retained in *L. bicolor*, where they might facilitate intercellular penetration of living roots. Both brown rot species lacked GH7 (endoglucanase/cellobiohydrolase CBHI), and GH61 genes, with unknown function but recently implicated in oxidative attack on polysaccharides (*23*), were reduced. Interestingly, GH6 (cellobiohydrolase CBHII) and cellulose binding modules (CBM1), absent from *P. placenta* (*13*), were present in *S. lacrymans*. One CBM was associated with an iron reductase in a gene (452187) originally derived from a cellobiose dehydrogenase (fig. S5).

The general utility of the conserved suite of glycoside hydrolase genes in wood decay by *S. lacrymans* was supported by transcriptomic and proteomic analysis. Carbohydrate active enzymes accounted for 50% of proteins

identified (table S14) and 33.9% of transcripts regulated more than 20-fold by *S. lacrymans* growing on pine wood compared with glucose medium (fig. S4). Cellulose-, pectin- and hemicellulose-degrading enzymes (GH families 5, 61, 3 and 28) were prominent, and GH5 endoglucanase (Prot id: 433209) and GH74 endoglucanase/xyloglucanase (453342) were upregulated >100-fold.

We conclude that brown rot fungi have cast off the energetically expensive apparatus of ligninolysis and acquired alternative mechanisms of initial attack. Wood decomposition by *S. lacrymans* may involve metabolically driven non-enzymatic disruption of lignocellulose with internal breakage of cellulose chains by highly localised ·OH radical action. Mycelia in split plates mimicking realistic nutrient heterogeneity (fig. S1), produced variegatic acid (VA), an iron-reducing phenolate (Fig. 2, A to C) via the Boletales atromentin pathway, recruited in *S. lacrymans* for the Fenton's reaction. The genome was rich in secondary metabolism genes (table S15), including a putative atromentin locus (*24*). Mycelium imports amino acids to sites of wood colonisation (*25*) , consistent with observed upregulation of oligopeptide transporters on wood (table S21). Localising variegatic acid production to well resourced parts of the mycelium could enhance Fenton's chemistry in contact with wood.

Wood colonisation is presumably followed by co-ordinated induction of the decay machinery revealed in the wood-induced transcriptome (Fig. 3 and fig. S4). Glycoside hydrolases and oxidoreductases accounted for 20.7% of transcripts accumulating > 4-fold on wood relative to glucose medium (fig. S4 and table S12). Iron reduction mechanisms included an enzyme harboring a C-terminal cellulose binding module (Prot id 452187) (fig. S10), upregulated 122 fold on wood substrate (fig. S4 and table S12). This enzyme, present in *Ph.chrysosporium* but absent from *P. placenta* (*26*), is a potential docking mechanism for localizing iron reductase activity, and hence ·OH generation, on the surface of microcrystalline cellulose. Cellulose-targeted iron reduction, combined with substrate induction of variegatic acid biosynthesis, might explain the unique ability of brown rot fungi in Boletales to degrade unassociated microcrystalline cellulose, without the presence of lignin (*27*).

Thus comparative genomics helps us understand the molecular processes of forest soil fungi that drive the element cycles of forest biomes (*28*). Sequenced forest Agaricomycetes revealed shared patterns of gene family contractions and expansions associated with emergences of both brown rot saprotrophy and ectomycorrhizal symbiosis. In Boletales, loss of aggressive ligninolysis might have permitted brown rot transitions to biotrophic ectomycorrhiza, promoted in soils impoverished in nitrogen by brown rot residues, and by the nutritional advantage conferred by the connection to a mycorrhizal network. *S.lacrymans* and other fungi cultured with conifer roots (*29*), ensheath *Pinus sylvestris* roots with a mantle-like layer (fig. S6), suggesting nutrient exchange.

The chronology of divergences in extant fungal nutritional mode (fig. 1A) matches the predicted major diversification in conifers (*18*), suggesting that the boreal forest biome may have originated via genetic coevolution of above and belowground biota.

References and Notes

1. F. Martin et al., Sequencing the fungal tree of life. *New Phytol.* Doi 1111/j.1469-8137.2011.03688.x (2011).
2. F. Martin, in *Biology of the Fungal Cell*, R. J. Howard, N. A. R. Gow, Eds. (Springer Berlin Heidelberg, 2007), vol. 8, pp. 291-308.
3. R. L. Gilbertson, Wood rotting fungi of North America. *Mycologia* **72**, 1-49 (1980).
4. D. S. Hibbett, M. J. Donoghue, Analysis of correlations among wood decay mechanisms, mating systems, and substrate ranges in homobasidiomycetes. *Syst. Biol.* **50**, 215 (2001).
5. K.-E. Eriksson, R. A. Blanchette, P. Ander, *Microbial and enzymatic degradation of wood and wood components*. (Springer-Verlag, Berlin; New York, 1990).
6. B. D. Lindahl *et al.*, Spatial separation of littler decomposition and mycorrhizal nitrogen uptake in a boreal forest. *New Phytol.* **173**, 611 (2007).
7. R. R. Northup, Z. Yu, R. A. Dahlgren, K. A. Vogt, Polyphenol control of nitrogen release from pine litter. *Nature* **377**, 227 (1995).
8. B. Goodell *et al.*, Low molecular weight chelators and phenolic compounds isolated from wood decay fungi and their role in the fungal biodegradation of wood. *J. Biotechnol.* **53**, 133 (1997).
9. T. Shimokawa, M. Nakamura, N. Hayashi, M. Ishihara, Production of 2,5-dimethoxyhydroquinone by the brown-rot fungus *Serpula lacrymans* to drive extracellular Fenton reaction. *Holzforschung* **58**, 305 (2005).
10. V. Arantes, A. Milagres, T. Filley, B. Goodell, Lignocellulosic polysaccharides and lignin degradation by wood decay fungi: the relevance of nonenzymatic fenton-based reactions. *J. Ind. Microbiol. Biotechnol.* **38**(4), 541 (2011).
11. S. F. Curling, C. A. Clausen, J. E. Winandy, Experimental method to quantify progressive stages of decay of wood by basidiomycete fungi. *Int. Biodeterioration Biodegradation* **49**, 13 (2002).
12. M. Binder, D. S. Hibbett, Molecular systematics and biological diversification of Boletales. *Mycologia* **98**, 971 (2006).
13. D. Martinez *et al.*, Genome, transcriptome, and secretome analysis of wood decay fungus *Postia placenta* supports

unique mechanisms of lignocellulose conversion. *Proc. Natl. Acad. Sci. U.S.A* **106**, 1954 (2009).
14. F. Martin *et al.*, Périgord black truffle genome uncovers evolutionary origins and mechanisms of symbiosis. *Nature* **464**, 1033 (2010).
15. F. Martin *et al.*, The genome of *Laccaria bicolor* provides insights into mycorrhizal symbiosis. *Nature* **452**, 88 (2008).
16. D. Martinez *et al.*, Genome sequence of the lignocellulose degrading fungus *Phanerochaete chrysosporium* strain RP78. *Nat. Biotech.* **22**, 695 (2004).
17. M. Binder *et al.*, Amylocorticiales ord. nov. and Jaapiales ord. nov.: Early diverging clades of Agaricomycetidae dominated by corticioid forms. Mycologia **102**, 865 (2010).
18. A. J. Eckert, B. D. Hall, Phylogeny, historical biogeography, and patterns of diversification for Pinus (Pinaceae): Phylogenetic tests of fossil-based hypotheses. *Mol. Phylogenet. and Evol.* **40**, 166 (2006).
19. H. Kauserud *et al.*, Asian origin and rapid global spread of the destructive dry rot fungus *Serpula lacrymans*. *Mol. Ecol.* **16**, 3350 (2007).
20. O. Schmidt, Molecular methods for the characterization and identification of the dry rot fungus *Serpula lacrymans*. *Holzforschung* **54**, 221 (2000).
21. Materials and methods are available as supporting material on *Science* Online.
22. B. L. Cantarel *et al.*, The Carbohydrate-Active EnZymes database (CAZy): An expert resource for glycogenomics. *Nucleic Acids Res.* **37**, D233 (2009).
23. G. Vaaje-Kolstad *et al.*, An oxidative enzyme boosting the enzymatic conversion of recalcitrant polysaccharides. *Science* **330**, 219 (2010).
24. P. Schneider, S. Bouhired, D. Hoffmeister, Characterization of the atromentin biosynthesis genes and enzymes in the homobasidiomycete *Tapinella panuoides*. *Fungal Genet. Biol.* **45**, 1487 (2008).
25. M. Tlalka, M. Fricker, S. Watkinson, Imaging of long-distance α-aminoisobutyric acid translocation dynamics during resource capture by *Serpula lacrymans*. *Appl. Environ. Microbiol.* **74**, 2700 (2008).
26. A. Vanden Wymelenberg *et al.*, Comparative transcriptome and secretome analysis of wood decay fungi *Postia placenta* and *Phanerochaete chrysosporium*. *Appl. Environ. Microbiol.* **76**, 3599 (2010).
27. T. Nilsson, J. Ginns, Cellulolytic activity and the taxonomic position of selected brown-rot fungi. *Mycologia* **71**, 170 (1979).
28 B. O. Lindahl, A. F. S. Taylor, R. D. Finlay, Defining nutritional constraints on carbon cycling in boreal forests - Towards a less 'phytocentric' perspective. *Plant Soil* **242**, 123 (2002).
29. R. Vasiliauskas, A. Menkis, R. D. Finlay, J. Stenlid, Wood-decay fungi in fine living roots of conifer seedlings. *New Phytol.* **174**, 441 (2007).
30. J. Sambrook, D.W. Russell, 3rd Edn (Cold Spring Harbor Laboratory Press, NY, 2001).
31. D.B. Jaffe *et al.*, *Genome Res.* **13**, 91 (2003).
32. S. Kurtz S *et al.*, *Genome Biol.* **5**, R12 (2004).
33. X. Huang, A. Madan, *Genome Res.* **9**, 868 (1999).
34. A.F.A. Smit, R. Hubley, P. Green, *RepeatMasker Open-3.0*. 1996-2010.
35. J. Jurka *et al.*, *Genome Res.* **110**, 462 (2005).
36. T.M. Lowe TM, S.R. Eddy, *Nucleic Acids Res.* **25**(5), 955 (1997).
37. A.A. Salamov AA, V.V. Solovyev, *Genome Res.* **10**, 516 (2000).
38. K. Isono, J.D. McIninch JD, M. Borodovsky, *DNA Res.* **1**(6), 263 (1994).
39. E. Birne, R. Durbin, *Genome Res.* **10**, 547 (2000).
40. W.J. Kent, *Genome Res.* **12**(4), 656 (2002).
41. H. Nielsen *et al.*, *Protein Engineering* **10**, 1 (1997).
42. K. Melen K, A. Krogh A, G. von Heijne, *J. Mol. Biol* **327**(3), 735 (2003).
43. E.M. Zdobnov, R. Apweiler, *Bioinformatics* **17**, 847 (2001).
44. S.F. Altschul *et al*., *J. Mol. Biol. **215***, 403 (1990).
45. M. Kanehisa *et al*., *Nucleic Acids Res.* **36**, D480 (2008).
46. E.V. Koonin *et al.*, *Genome Biol.* **5**, R7 (2004).
47. A.J. Enright, S. Van Dongen, C.A. Ouzounis, *Nucleic Acids Res.* **30**, 1575 (2002).
48. T. De Bie, *et al.*, *Bioinformatics* **22**, 1269 (2006).
49. D.R. Maddison, W.P. Maddison, MacClade 4 Sunderland, Massachusetts: Sinauer Associates (2005).
50. A.J. Drummond, A. Rambaut, *BMC Evolutionary Biol.* **7**, 214 (2007).
51. M. Binder *et al.*, *Syst Biodiversity* **3**, 113 (2005).
52. P.B. Matheny, *et al.*, *Mycologia* **98**, 982 (2006).
53. D.S. Hibbett, D. Grimaldi, M.J. Donoghue, *Am. J. Bot.* **84**, 981 (1997).
54. B.A. LePage *et al.*, *Am. J. Bot.* **84**, 470 (1997).
55. A. Rambaut, A.J. Drummond, Tracer v1.4 http://beast.bio.ed.ac.uk/Tracer (2007).
56. K. Katoh *et al.*, *Nucleic Acids Res.* **33**, 511 (2005).
57. F. Abascal, R. Zardoya, D. Posada, *Bioinformatics* **21**, 2104 (2005).
58. A. Stamatakis, P. Hoover, J. Rougemont, *Syst. Biol.* **75**(5), 758 (2008).
59. T.Y. James *et al.*, *Nature* **443**, 818 (2006).
60. D. Durand, B.V. Halldorsson, B. Vernot, *J. Comp. Biol.* **13**(2), 320 (2006).
61. B. Vernot *et al.*, *J. Comp. Biol.* **15**(8), 981 (2008).
62. Y. Benjamini, Y. Hochberg, *J. Roy. Statist. Soc. B (Methodological)* **57**, 289 (1995).

63. A. Bensadoun, D. Weinstein, *Anal. Biochem.* **70**, 241 (1976).
64. H.Y. Yeang, F. Yusof, L. Abdullah, *Anal. Biochem.* **265**, 381 (1998).
65. D. Fragner *et al.*, *Electrophoresis* **30**(14), 2431 (2009).
66. B.J. Cargile *et al.*, *J. Proteome Res.* **3**, 112 (2004).
67. J. Krijgsveld *et al.*, *J. Proteome Res.* **5**, 1721 (2006).
68. J. Havlis *et al.*, *Anal. Chem.* **75**(6), 1300 (2003).
69. J. Rappsilber, Y. Ishihama, M. Mann *Anal. Chem.* **75**, 663 (2003).
70. C.L. Chepanoske *et al.*, *Mass Spectrom.* **19**, 9 (2005).
71. I. Shadforth *et al.*, *Rapid Commun. Mass Spectrom.* **19**, 3363 (2005).
72. M. Gill, W. Steglich, *Prog. Chem. Org. Nat. Prod.* **51**, 1 (1987).
73. L.L. Stookey, *Anal. Chem.* **42**, 779 (1979).
74. D.W. Malloch, K. A. Pirozynski, P. H. Raven. *Proc. Natl. Acad. Sci. USA* **77**, 2113 (1980).
75. J.W.G. Cairney, *Naturwissenschaften* **87**, 467 (2000)
76. X.-Q. Wang, D.C.Tank, T. Sang, *Mol. Biol. Evol.* **17**, 773 (2000).
77. D.S. Hibbett, P. B. Matheny, 2009. *BMC Biol.* **7**, 13 (2009).
78. A.M. Bresinsky *et al.*, *Plant Biol.* **1**, 327 (1999).
79. F. Florindo, A. K. Cooper, P. E. O'Brien, *Palaeogeogr. Palaeoclimatol. Palaeoecol.* **198**, 1 (2003).
80. L.A. Lawyer, L. M. Gahagan, *Palaeogeogr. Palaeoclimatol. Palaeoecol.* **198**, 11 (2003).
81. L.G. Cook, M. D. Crisp. 2005. *Proc. Royal Soc. B, Biol. Sci.* **272**, 2535 (2005).
82. R.A. Ohm, *et al.*, *Nat. Biotechnol.* **28**, 957 (2010).
83. D.R. Schmidhalter, G. Canevascini, *Archiv. Biochem. Biophys.* **300**, 551 (1993).
84. T. Kajisa, K. Igarashi, M. Samejima, *J. Wood Sci.* **55**, 376 (2009).
85. S. Nagendran, *et al.*, *Fungal Genet. Biol.* **46**, 427 (2009).
86. A. Bresinsky, *Z Naturforsch* **28**c, 627 (1973).
87. P. Aqueveque, T. Anke, O. Sterner, *Z Naturforsch* **57**, 257 (2002).
88. I.W. Farrell, *et al.*, *J. Chem. Soc. Perkin Trans.* I, 2642 (1973).
89. D. Hoffmeister, N.P. Keller, *Nat. Prod. Rep.* **24**, 393 (2007).

Acknowledgements: Drs J. Schilling, U Minnesota and Dr D. Barbara, U Warwick critically reviewed the manuscript, Tony Marks designed graphics, B Wackler and M. Zomorrodi gave technical assistance. Assembly and annotations of *S.lacrymans* genomes are available at http://www.jgi.doe.gov/Serpula and DDBJ/EMBL/GenBank, accessions AECQB00000000 and AEQC00000000. Complete microarray expression dataset is available at the Gene Expression Omnibus (http://www.ncbi.nml.nhi.gov/geo/) accession GSE27839. The work conducted by the U.S. Department of Energy Joint Genome Institute and supported by the Office of Science of the U.S. Department of Energy under Contract No. DE-AC02-05CH11231. Further financial support is acknowledged as supporting material on *Science* online.

Supporting Online Material

www.sciencemag.org/cgi/content/full/science.1205411/DC1
Materials and Methods
SOM Text
Figs. S1 to S6
Tables S1 to S15
References (*30–89*)

10 March 2011; accepted 20 June 2011
Published online 14 July 2011; 10.1126/science.1205411

Fig. 1. Molecular phylogeny and lignocellulose active gene evolution in the Agaricomycetes. (**A**) Chronogram of Agaricomycetes inferred from a combined six-gene data set using Bayesian relaxed molecular clock analyses. Time divergence estimates (in Mya) are presented as 95% highest posterior density (HPD) node bars in light blue color, which describe the upper and lower boundaries of time estimates, and as mean node ages (numbers in bars). The HPD of nodes that were calibrated with fossil ages are in red color and the *Serpula-Austropaxillus* split is highlighted by a black node bar. The numbering of nodes in bold type corresponds to the tMRCA statistics (time to Most Recent Common Ancestor) summarized in table S20. (**B** and **C**) Patterns of gene duplication and loss in 12 lignocelluloseactive CAZy (B) and 7 oxidoreductase (C) gene families estimated by gene tree/species tree reconciliation analysis (fig S3). Red, blue, and black branches indicate lineages with net expansions, net contractions, or no change in copy number (respectively). Numbers at nodes and along branches indicate estimated copy numbers for ancestral species, and ranges of gains and losses (respectively), estimated using 90% and 75% bootstrap thresholds for gene trees in reconciliations. Bars indicate copy numbers in sampled genomes.

Fig. 2. (**A**) Proposed chemical reaction demonstrating iron redox cycling by *S. lacrymans* secondary products, (**B**) Comparison of HPLC chromatograms of *S. lacrymans* ethyl acetate extracts as a function of nitrogen supply. Red trace: nitrogen rich medium (+N), black trace: nitrogen depleted minimal medium (-N). The identity of the compounds was confirmed by mass spectrometry and by their UV-VIS spectrum (1: variegatic acid, 2: xerocomic acid, 3: atromentic acid), (**C**) Iron reduction capacity of *S. lacrymans* ethyl acetate extracts (60% variegatic acid, 15% xerocomic acid) measured by the Ferrozine assay (*21*) and compared with 2,3-

dihydroxybenzoic acid (DHBA), a redox chelator used to stimulate Fenton systems.

Fig. 3. Schematic overview of the proposed mechanism of wood decay by *S. lacrymans*. Scavenging mycelium colonises a new food source inducing variegatic acid (VA) production and expression of oxidoreductase enzymes which drive hydroxyl radical attack on the lignocellulose composite. Carbohydrate active enzymes (CAZy) gain access to the weakened composite structure and breakdown accessable carbohydrates. Cellulose-binding iron reductase targets ·OH-generating Fenton's reaction on cellulose chains, releasing chain ends for hydrolysis and assimilation. IR = iron reductase, HQ = hydroxyquinones, CBM = cellulose binding module.

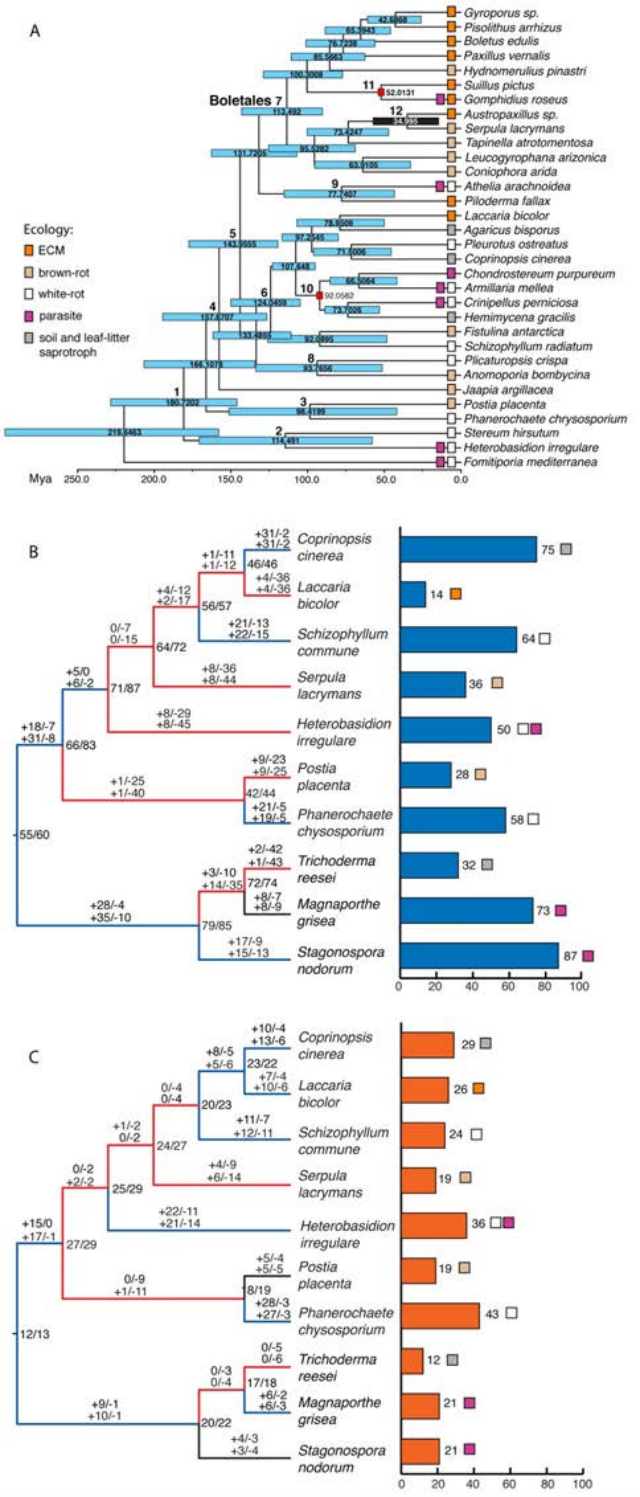
A
Gyroporus sp.
Pisolithus arrhizus
Boletus edulis
Paxillus vernalis
Hydnomerulius pinastri
Suillus pictus
Gomphidius roseus
Austropaxillus sp.
Serpula lacrymans
Tapinella atrotomentosa
Leucogyrophana arizonica
Coniophora arida
Athelia arachnoidea
Piloderma fallax
Laccaria bicolor
Agaricus bisporus
Pleurotus ostreatus
Coprinopsis cinerea
Chondrostereum purpureum
Armillaria mellea
Crinipellus perniciosa
Hemimycena gracilis
Fistulina antarctica
Schizophyllum radiatum
Plicaturopsis crispa
Anomoporia bombycina
Jaapia argillacea
Postia placenta
Phanerochaete chrysosporium
Stereum hirsutum
Heterobasidion irregulare
Fomitiporia mediterranea
Boletales 7
Ecology:
ECM
brown-rot
white-rot
parasite
soil and leaf-litter saprotroph
Mya
250.0
200.0
150.0
100.0
50.0
0.0
B
Coprinopsis cinerea
Laccaria bicolor
Schizophyllum commune
Serpula lacrymans
Heterobasidion irregulare
Postia placenta
Phanerochaete chysosporium
Trichoderma reesei
Magnaporthe grisea
Stagonospora nodorum
75
14
64
36
50
28
58
32
73
87
0
20
40
60
80
100
C
Coprinopsis cinerea
Laccaria bicolor
Schizophyllum commune
Serpula lacrymans
Heterobasidion irregulare
Postia placenta
Phanerochaete chysosporium
Trichoderma reesei
Magnaporthe grisea
Stagonospora nodorum
29
26
24
19
36
19
43
12
21
21
0
20
40
60
80
100

A

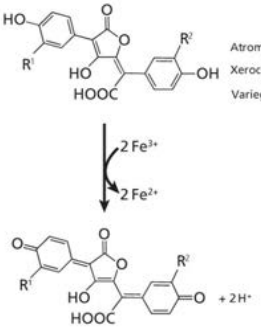
HO
R1
HO
HOOC
O
O
R2
OH
Atromentic acid: R1 = R2 = H
Xerocomic acid: R1 = OH, R2 = H
Variegatic acid: R1 = R2 = O H
2 Fe3+
2 Fe2+
+ 2H+

B

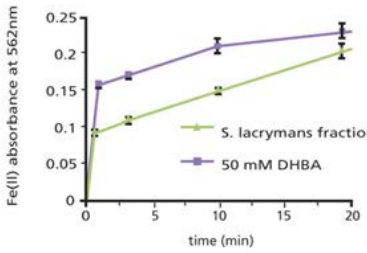
Fe(II) absorbance at 562nm
0.25
0.2
0.15
0.1
0.05
0
0
5
10
15
20
time (min)
S. lacrymans fraction
50 mM DHBA

C

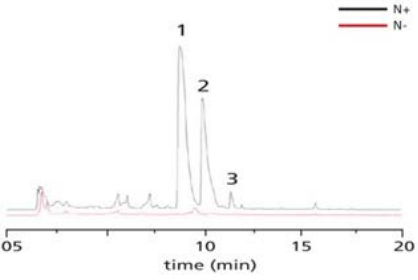
N+
N-
1
2
3
05
10
15
20
time (min)

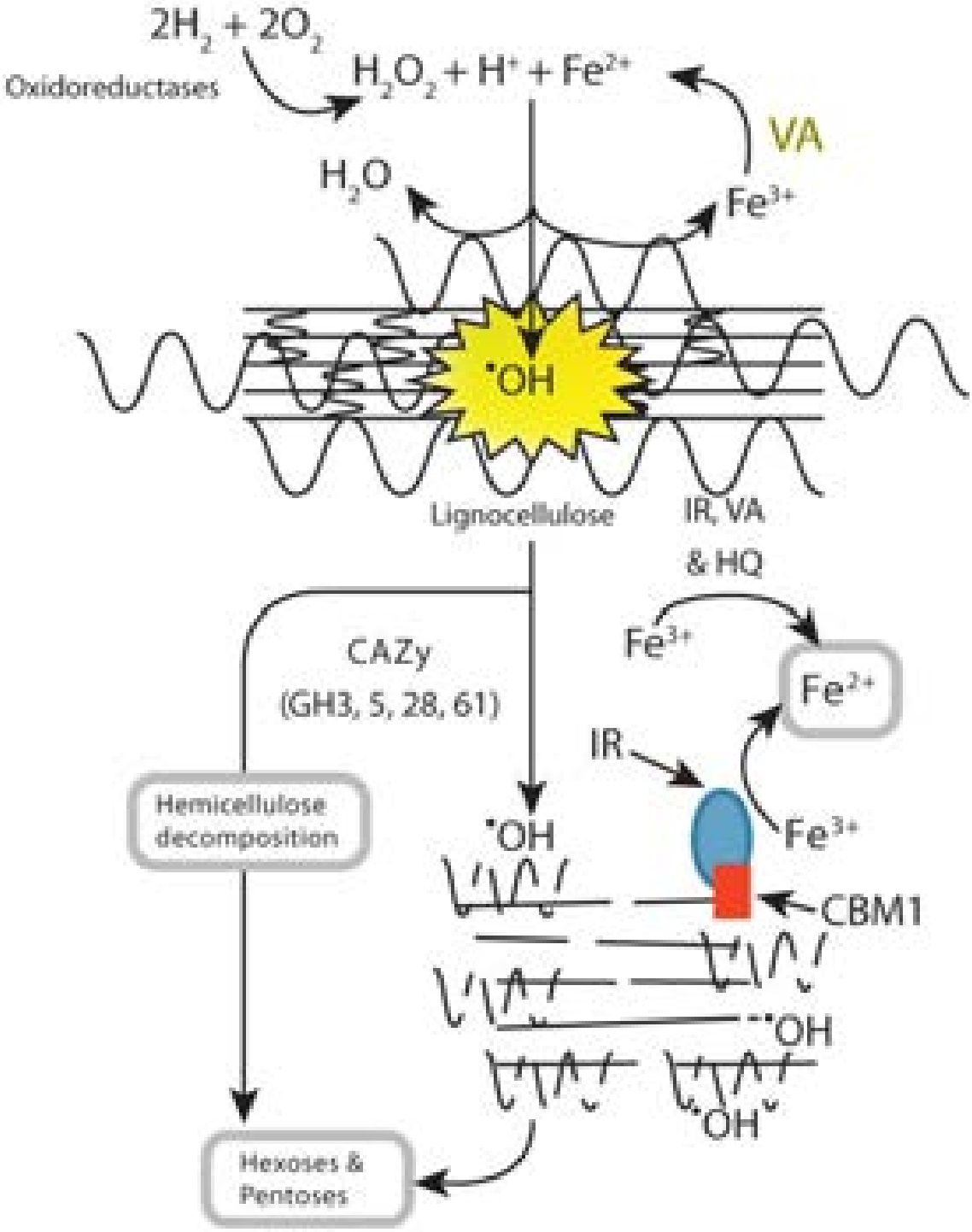
$2H_2 + 2O_2$
Oxidoreductases
$H_2O_2 + H^+ + Fe^{2+}$
VA
H_2O
Fe^{3+}
·OH
Lignocellulose
IR, VA
& HQ
Fe^{3+}
Fe^{2+}
CAZy
(GH3, 5, 28, 61)
IR
Hemicellulose
decomposition
·OH
Fe^{3+}
CBM1
·OH
·OH
Hexoses &
Pentoses